Cell Metabolism
Short Article

The IRP1-HIF-2α Axis Coordinates Iron and Oxygen Sensing with Erythropoiesis and Iron Absorption

Sheila A. Anderson,[1,6] Christopher P. Nizzi,[1,6] Yuan-I. Chang,[2,6] Kathryn M. Deck,[1] Paul J. Schmidt,[5] Bruno Galy,[4] Alisa Damnernsawad,[2] Aimee T. Broman,[3] Christina Kendziorski,[3] Matthias W. Hentze,[4] Mark D. Fleming,[5] Jing Zhang,[2,*] and Richard S. Eisenstein[1,*]

[1]Department of Nutritional Sciences
[2]McArdle Laboratory for Cancer Research
[3]Biostatistics and Medical Informatics
University of Wisconsin-Madison, Madison, WI 53706, USA
[4]European Molecular Biology Laboratory, Meyerhofstrasse 1, 69117 Heidelberg, Germany
[5]Department of Pathology, Boston Children's Hospital and Harvard Medical School, 320 Longwood Avenue, Boston, MA 02115, USA
[6]These authors contributed equally to this work
*Correspondence: zhang@oncology.wisc.edu (J.Z.), eisenste@nutrisci.wisc.edu (R.S.E.)
http://dx.doi.org/10.1016/j.cmet.2013.01.007

SUMMARY

Red blood cell production is a finely tuned process that requires coordinated oxygen- and iron-dependent regulation of cell differentiation and iron metabolism. Here, we show that translational regulation of hypoxia-inducible factor 2α (HIF-2α) synthesis by iron regulatory protein 1 (IRP1) is critical for controlling erythrocyte number. IRP1-null (*Irp1*$^{-/-}$) mice display a marked transient polycythemia. HIF-2α messenger RNA (mRNA) is derepressed in kidneys of *Irp1*$^{-/-}$ mice but not in kidneys of *Irp2*$^{-/-}$ mice, leading to increased renal erythropoietin (Epo) mRNA and inappropriately elevated serum Epo levels. Expression of the iron transport genes *DCytb*, *Dmt1*, and ferroportin, as well as other HIF-2α targets, is enhanced in *Irp1*$^{-/-}$ duodenum. Analysis of mRNA translation state in the liver revealed IRP1-dependent dysregulation of HIF-2α mRNA translation, whereas IRP2 deficiency derepressed translation of all other known 5′ iron response element (IRE)-containing mRNAs expressed in the liver. These results uncover separable physiological roles of each IRP and identify IRP1 as a therapeutic target for manipulating HIF-2α action in hematologic, oncologic, and other disorders.

INTRODUCTION

Erythropoiesis is a dynamic process regulated through the complex interplay of cytokines, the availability of nutrients, and the cellular environment of erythroid progenitors (Hattangadi et al., 2011). The level of circulating erythrocytes must be tightly controlled because a deficiency leads to anemia and that the consequent negative impact of hypoxic stress, whereas chronically high levels can lead to hyperviscosity and potentially lethal thrombotic events (Lee and Percy, 2011). Excess accumulation of erythrocytes, referred to as polycythemia or erythrocytosis, occurs physiologically, as in an adjustment to high altitude, or pathologically, because of intrinsic abnormalities in erythroid precursors or as a consequence of inappropriately high expression of erythropoietin (Epo) (Lee and Percy, 2011). Critical factors governing red cell formation include oxygen and iron sensing, particularly through the transcription factor hypoxia-inducible factor 2α (HIF-2α), which regulates Epo expression as well as the expression of multiple other genes required for iron assimilation (Gruber et al., 2007; Haase, 2010; Mastrogiannaki et al., 2009; Scortegagna et al., 2005; Shah et al., 2009; Taylor et al., 2011). Elucidating the mechanisms regulating Epo production and action is relevant for understanding the etiology of, and to design treatments for, common diseases and pathological states ranging from the anemia of prematurity to the anemias associated with inflammation, cancers, aging, and renal failure (Strauss, 2010; Weiss and Goodnough, 2005).

HIFs are heterodimeric transcription factors regulated by oxygen and iron (Majmundar et al., 2010; Prabhakar and Semenza, 2012). HIFs contain a subunit from a family of inducibly degraded α proteins that have overlapping but unique physiological and pathophysiological roles. The key role of HIF-2α in erythropoiesis has been demonstrated, in part, through the discovery of human HIF-2α gain-of-function mutations that cause polycythemia (Lee and Percy, 2011). Dysregulation of HIF-2α is also implicated in human cancers (Franovic et al., 2009; Keith et al., 2012; Tong et al., 2011). Although much previous work has focused on the regulation of HIF action through oxygen- and iron-mediated protein degradation, recent work with cultured cells has revealed new mechanisms for HIF regulation, including programmed changes in their synthesis (Sanchez et al., 2007; Tong et al., 2011; Young et al., 2008; Zimmer et al., 2010). Thus, physiological control of HIF-2α function and its dysregulation in disease may arise because of adaptive or maladaptive changes in HIF-2α synthesis.

Iron regulatory protein 1 (IRP1) and IRP2 are central regulators of cellular iron metabolism in metazoans (Anderson et al., 2012; Hentze et al., 2010). IRPs control the fate of messenger RNAs

(mRNAs) that encode proteins, including HIF-2α, involved in iron metabolism or the adaptive responses to iron deficiency. The finding that a deficiency of IRP2, but apparently not of IRP1, leads to dysregulated iron metabolism (Cooperman et al., 2005; Galy et al., 2005b; Meyron-Holtz et al., 2004) has led to the view that IRP1 lacks a unique role in iron metabolism. However, the fact that the Fe-S switch mechanism controlling IRP1 allows for the inactivation of its RNA binding in hypoxia, in contrast to IRP2, which is activated, suggests otherwise (Anderson et al., 2012). Thus, as is the case for HIF-2α mRNA in cultured cells, translation of mRNAs preferentially repressed by IRP1 would be enhanced in hypoxia (Zimmer et al., 2008). These findings suggest that an IRP1-HIF-2α regulatory axis may be a critical component of systemic mechanisms controlling erythrocyte number as well as tissue responses to iron deficiency and hypoxic stress.

Here, we studied the impact of IRP1 deficiency on the function of HIF-2α in erythropoiesis and duodenal iron absorption. Our study reveals that, through its regulation of HIF-2α expression, IRP1 has a key role linking erythropoiesis and dietary iron absorption with iron and oxygen sensing, a function not attributed to IRP2. The IRP1-HIF-2α axis provides new therapeutic targets for modulating the response of cells to altered iron or oxygen levels in a wide array of hematologic and oncologic diseases.

RESULTS

Polycythemia and Extramedullary Erythropoiesis in IRP1-Deficient Mice

In the process of elucidating the unique physiological functions of IRP1 and IRP2, we observed that young IRP1-null (*Irp1*$^{-/-}$) mice frequently had reddened paws around 5 weeks of age (Figure 1A), reminiscent of the "plethora" seen in human patients with polycythemias. Accordingly, we found that hematocrit, red cell number, and hemoglobin are elevated in *Irp1*$^{-/-}$ mice between 4 and 6 weeks of age (Figure 1B, and Table S1 available online). The elevated hematocrit level is similar to that observed in humans with HIF-2α gain-of-function mutations (Lee and Percy, 2011). *Irp1*$^{-/-}$ spleens are most enlarged at 4 and 5 weeks of age but thereafter normalize (Figures 1C and 1D). Serum and tissue iron parameters are indicative of iron redistribution to the erythron (Table S2). When *Irp1*$^{-/-}$ mice reach 8 weeks of age, the hematocrit remains elevated although there is substantial variability from animal to animal such that only approximately one-third of the animals have elevated hematocrit. At this age, the hematocrit of *Irp1*$^{-/-}$ and *Irp1*$^{+/+}$ is not statistically different ($p = 0.058$), illustrating the age-dependent effect of IRP1 deficiency (Figure 1B).

Spleens from 5-week-old *Irp1*$^{-/-}$ mice demonstrated an altered architecture, characterized by a decreased white pulp and a substantially increased red pulp, signifying expanded erythropoiesis (Figure 1E). Immunohistochemistry for TfR1 (CD71) confirmed that the *Irp1*$^{-/-}$ splenic red pulp is distended by erythroblasts (Figure 1E). Maturing erythroblasts of different developmental stages were quantified by flow cytometry with the erythroid-specific marker Ter119 and with CD71 (Socolovsky et al., 2001). This analysis reveals the marked accumulation of erythroblasts in bone marrow and particularly in spleens of 5-week-old *Irp1*$^{-/-}$ mice (Figures 1F and 1G). The relative abundance of cells at different stages of erythroblast maturation was not altered in bone marrow (BM), whereas, in the *Irp1*$^{-/-}$ spleen, the distribution was skewed toward having more cells at stage II and fewer cells at stage IV (Figure 1H and Table S3). This altered pattern of maturation may reflect the response to Epo itself or to changes induced by the splenic microenvironment (Socolovsky et al., 2001). Interestingly, at 6 weeks of age, enhanced erythropoiesis was only observed in about one-quarter of the *Irp1*$^{-/-}$ mice, indicating an age-dependent compensation for the loss of IRP1 (Figures S1C and S1D).

To determine whether IRP1 deficiency caused a specific enhancement of erythropoiesis, the abundance of hematopoietic progenitors was determined. IRP1 deficiency does not appear to affect the abundance of primitive hematopoietic stem and progenitor cells ($Lin^{-}Sca1^{+}c\text{-}kit^{-}$ [LSK] cells) or myeloid progenitor cells in either the BM or the spleen (SP) (Figure 2A). Consistent with the flow cytometric analysis, early-stage myeloid progenitors formed similar numbers of colonies in vitro, irrespective of genotype (Figure 2B). In contrast, the primitive erythroid BFU-E and late-stage CFU-E progenitors were elevated in BM and particularly in SP of *Irp1*$^{-/-}$ mice, whereas progenitors for other hematopoietic lineages were not altered (Figures 2B and 2C). Then, we determined whether IRP1 deficiency affected the sensitivity of CFU-E cells to Epo. No such effect was observed (Figure 2D). Collectively, these findings reveal that IRP1 deficiency is associated with an age-dependent increase in erythropoiesis in young mice and not a general increase in hematopoiesis. We conclude that IRP1 has a previously unrecognized role as a regulator of erythropoiesis and that its dysregulation contributes to the development of polycythemia. The erythroid phenotype of IRP1 is distinct from that of IRP2 deficiency—e.g., microcytic anemia and erythropoietic protoporphyria (Cooperman et al., 2005; Galy et al., 2005b).

Enhanced Serum Epo and Erythroid Gene Expression in Spleen of *Irp1*$^{-/-}$ Mice

Given that HIF-2α is a major regulator of Epo gene transcription and that HIF-2α mRNA translation is a direct target of IRP action (Davis et al., 2011; Sanchez et al., 2007; Zimmer et al., 2008), Epo expression was examined in *Irp1*$^{-/-}$ mice. Epo expression is developmentally regulated after birth, reflecting the increased oxygen level relative to in utero levels, an increased demand for erythropoiesis, and a relative iron deficiency as the neonate grows (Lee and Percy, 2011). The maximal changes observed in erythropoiesis in *Irp1*$^{-/-}$ mice relative to *Irp1*$^{+/+}$ mice occurred at 5 weeks of age, which was coincident with the slowing of growth and the attendant increase in red blood cell mass as the animal reaches adult weight. To determine whether the effect was Epo-dependent, we measured serum Epo concentration in 4-, 5-, and 8-week-old mice. At 4 weeks, serum Epo concentration was high in *Irp1*$^{+/+}$ and *Irp1*$^{-/-}$ mice, most likely reflecting a physiologically appropriate erythropoietic drive in young mice (Figure 3A). However, at 5 weeks, when the difference in erythropoiesis is apparent in *Irp1*$^{-/-}$ mice, serum Epo level is 2- to 3-fold higher than in *Irp1*$^{+/+}$ mice. At this time, kidney Epo mRNA is increased by more than 8-fold in *Irp1*$^{-/-}$ animals (Figure 3B). Furthermore, expression of multiple genes involved in erythroid development, including globins and heme biosynthetic genes,

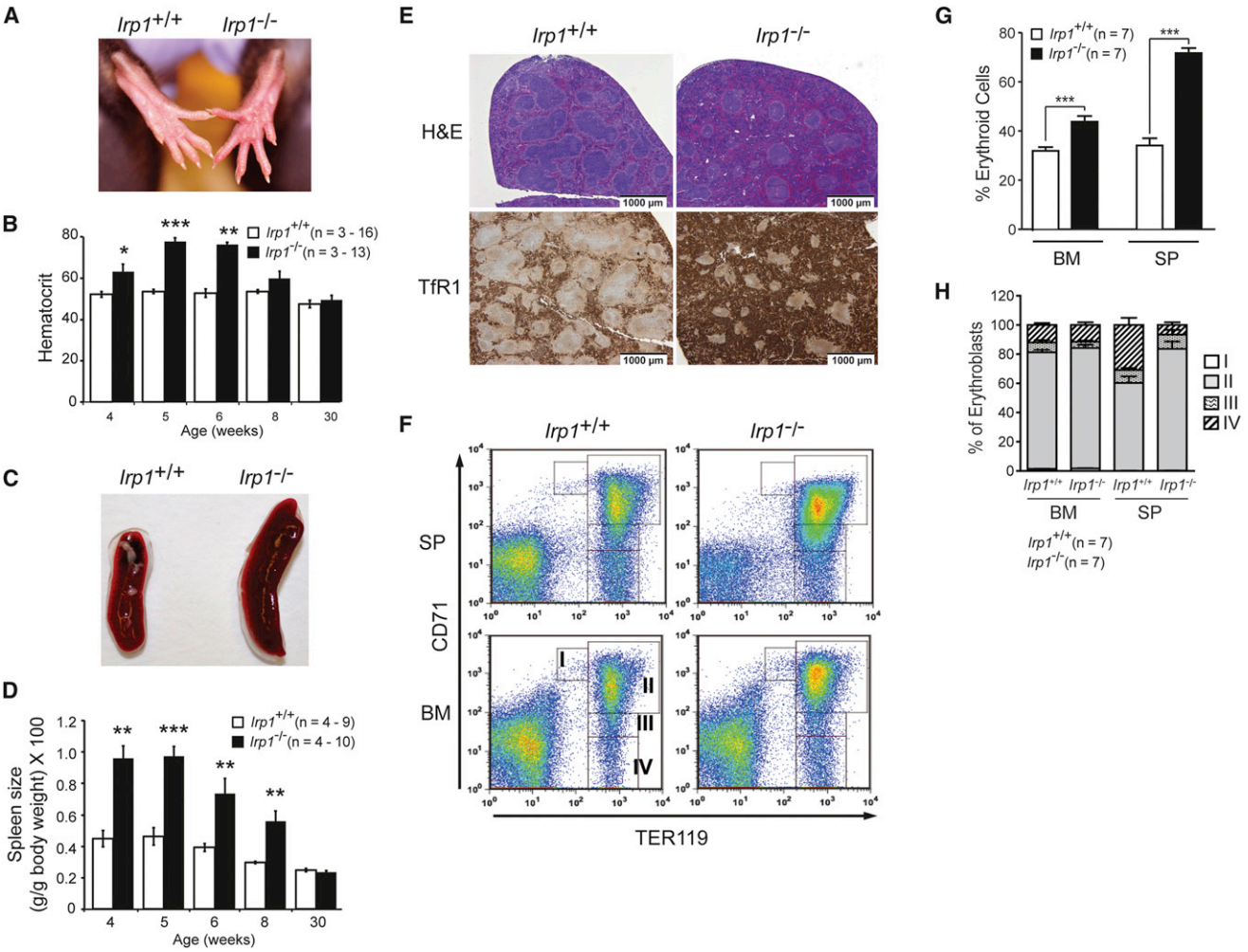

Figure 1. Polycythemia and Extramedullary Erythropoiesis in IRP1-Deficient Mice

(A) Rear paws showing greater redness in *Irp1*$^{-/-}$ mice.

(B) Hematocrit analysis for *Irp1*$^{+/+}$ and *Irp1*$^{-/-}$ mice. Samples were collected from the retroorbital sinus or by cardiac puncture and hematocrit was from CBC analysis. n = 2 for 30-week *Irp1*$^{+/+}$ mice.

See also Table S1.

(C) Spleens from 6-week-old wild-type (WT) and *Irp1*$^{-/-}$ mice.

(D) Spleen weight as a percent body weight as a function of age. n = 2 for 30-week *Irp1*$^{+/+}$ mice.

(E) Hematoxylin and eosin (H&E) staining (top) or immunohistochemistry for CD71(TfR1) (bottom) in spleens.

(F) Fluorescence-activated cell sorting (FACS) analysis of cells isolated from bone marrow (BM) and spleen (SP) with staining for the erythroid marker Ter119 and CD71 (TfR). The cell populations are separated into stage I –stage IV reflecting increasing differentiation of the erythroblasts as described (Socolovsky et al., 2001).

(G) Percentage of nucleated cells that are erythroblasts in BM and SP.

(H) Erythroblast differentiation state in BM and SP as determined by FACS. For panels (B), (D), (G), and (H), results are expressed as mean ± SEM. *, $p < 0.05$; **, $p < 0.01$; ***, $p < 0.001$. Unless noted, 5-week-old mice were used.

See also Tables S1, S3, and Figure S1.

was increased in *Irp1*$^{-/-}$ SP (Figure 3C), most likely reflecting an increased erythroblast number. Given that Epo promotes the expansion of BFU-E and CFU-E cells (Peslak et al., 2012), the rise in these erythroid progenitors in *Irp1*$^{-/-}$ mice at 5 weeks of age can be explained by an inability to suppress Epo expression.

Interestingly, serum Epo concentration at 8 weeks of age is persistently high in *Irp1*$^{-/-}$ mice. Given that erythropoiesis returns to normal by about 6 weeks in *Irp1*$^{-/-}$ mice (Figures S1C and S1D), it appears that erythroid differentiation has become desensitized to the elevated Epo. Epo resistance is clinically relevant in a number of chronic disease states and can be caused by iron deficiency, inflammatory cytokines, or a reduction of Epo-responsive, late-stage erythroid progenitors (Andrews and Bridges, 1998; Peslak et al., 2012; van der Putten et al., 2008). Because the reduction in transferrin iron in *Irp1*$^{-/-}$ mice (Table S2) does not appear to reach a level that impairs erythropoiesis, at least in vitro (Bullock et al., 2010), we conclude that other factors are most likely responsible. In summary, we

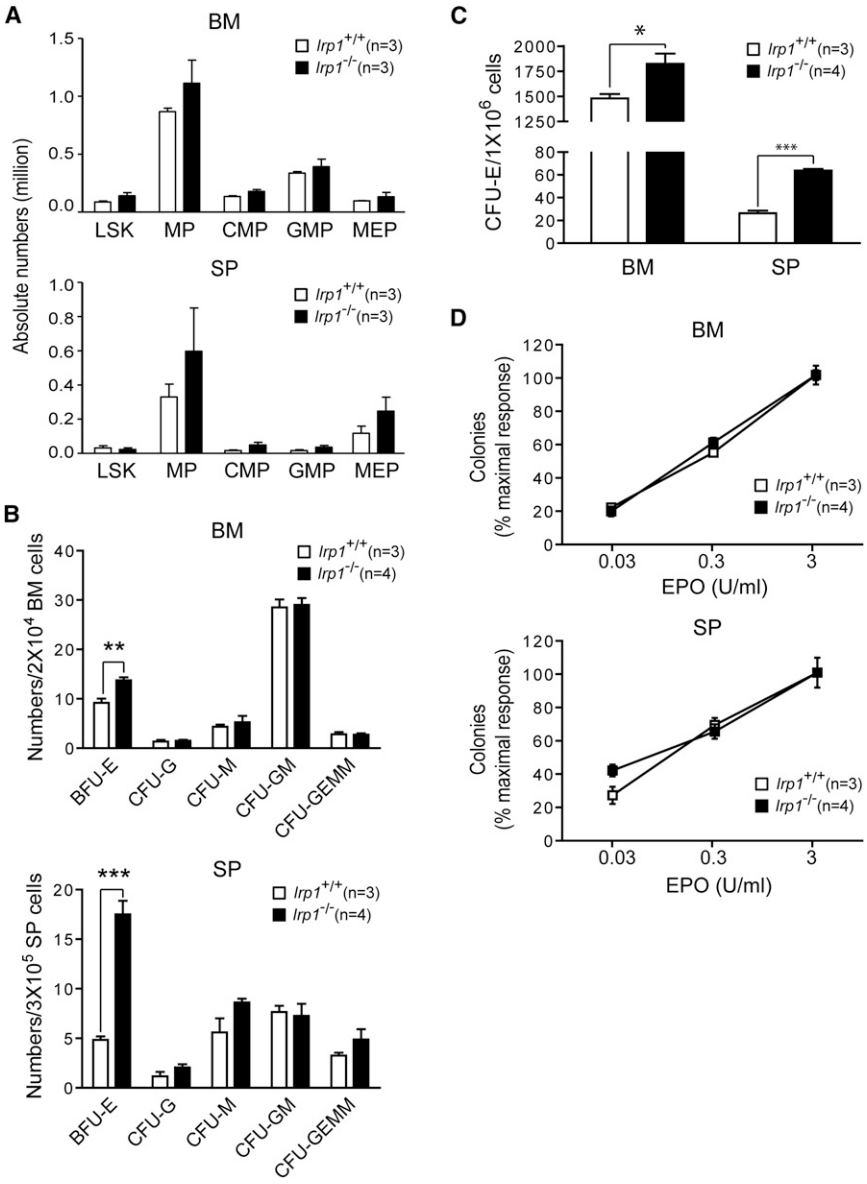

Figure 2. Specific Increase in Erythroid Progenitors in *Irp1*$^{-/-}$ Mice

(A) Abundance of myeloid progenitor cells (LSK, Lin$^-$Sca1$^+$c-kit$^-$; MP, myeloid progenitors; CMP, common myeloid progenitors; GMP, granulocyte macrophage progenitors; MEP, megakaryocyte erythroid progenitors) in SP and BM. For panels (B), (C) and (D), BM and SP cells were isolated from *Irp1*$^{+/+}$ and *Irp1*$^{-/-}$ mice and plated in duplicate in M3234 medium with 3 U/ml ([B] and [C]) or varying concentrations ([D]) of Epo.

(B) Average percentage of the maximum number of colonies formed in culture. For BFU-E (burst forming unit-erythroid), CFU-G (colony forming unit [CFU]-granulocyte), CFU-M (CFU-macrophage), CFU-GM (CFU-granulocyte-macrophage), and CFU-GEMM (CFU-granulocyte, erythroid, macrophage, megakaryocytic) colony formation, BM, and SP cells were plated in an M3434 medium and colonies were counted at day 7 after plating.

(C) CFU-E (CFU-erythroid) number in BM and SP cells.

(D) CFU-E number as a function of Epo concentration. Error bars show SEM. *, $p < 0.05$; **, $p < 0.01$; ***, $p < 0.001$. Mice were 5 weeks old.

conclude that, in young *Irp1*$^{-/-}$ mice, an unidentified developmental signal that normally acts through IRP1 to suppress HIF-2α synthesis is absent, leading to a failure to suppress Epo expression. As *Irp1*$^{-/-}$ mice age, one of many factors controlling Epo action or other aspects of erythropoiesis acts to limit red cell production because of IRP1 deficiency and compensates for the inappropriately high Epo level.

HIF-2α Hyperactivity in Duodenum of *Irp1*$^{-/-}$ Mice

HIF-2α induces transcription of the duodenal iron transporter genes in response to hypoxia or iron deficiency (Taylor et al., 2011). The mRNAs that encode key components of the apical (*DCytb* [*Cybrd1*] and *Dmt1* [*Slc11a2*]) and basolateral (ferroportin [*Slc40a1*]) iron transporters are significantly increased in *Irp1*$^{-/-}$ duodenal mucosal cells (Figure 3D). The preferential impact of IRP1 deficiency on the iron response element (IRE)-containing forms of DMT1 mRNA is consistent with this isoform being a target of HIF-2α action (Mastrogiannaki et al., 2009; Shah et al., 2009).

Using a transcriptomic approach, we found 25 genes that were differentially expressed between *Irp1*$^{+/+}$ and *Irp1*$^{-/-}$ duodenum (Figures 3E and S2). Among these genes are *DCytb* (*Cybrd1*) and *Dmt1* (*Slc11a2*). Multiple other molecular signatures emerged as well. First, expression of the prolyl hydroxylase *Egln3* mRNA (*Phd3* mRNA) that controls HIFα protein stability is increased in *Irp1*$^{-/-}$ duodenum (Figures 3D, 3E, and S2). EGLN3 is part of a feedback loop for HIF-2α, and the *Egln3* gene contains a bona fide hypoxia response element (Lee and Percy, 2011; Minamishima et al., 2009; Pescador et al., 2005). Second, induction of the amino acid transporter SLC38A1 and the enzyme gamma-glutamyl hydrolase (GGH) by iron deficiency requires HIF-2α (Taylor et al., 2011). Duodenal expression of both genes is increased in *Irp1*$^{-/-}$ mice (Figures 3D and 3E). Third, in addition to *DCytb*, *Dmt1*, ferroportin (*Slc40a1*), *Slc38a1, Ggh* and *Egln3*, the expression of *Pparg*, *Nt5E*, and *Snca* mRNAs are also altered in *Irp1*$^{-/-}$ duodenum (Figures 3E and S2). Each of these genes is either an HIF-2α target or responsive to the O_2 level (see Figure S2). Altogether, the polycythemia observed in *Irp1*$^{-/-}$ mice is linked with increases in HIF-2α activity and, as such, supports the notion that a loss of IRP1 is similar to an HIF-2α gain of function. On this basis, we conclude that IRP1 provides a critical link between the fundamental pathways of cellular iron and oxygen use and the systemic regulation of iron absorption and erythropoiesis.

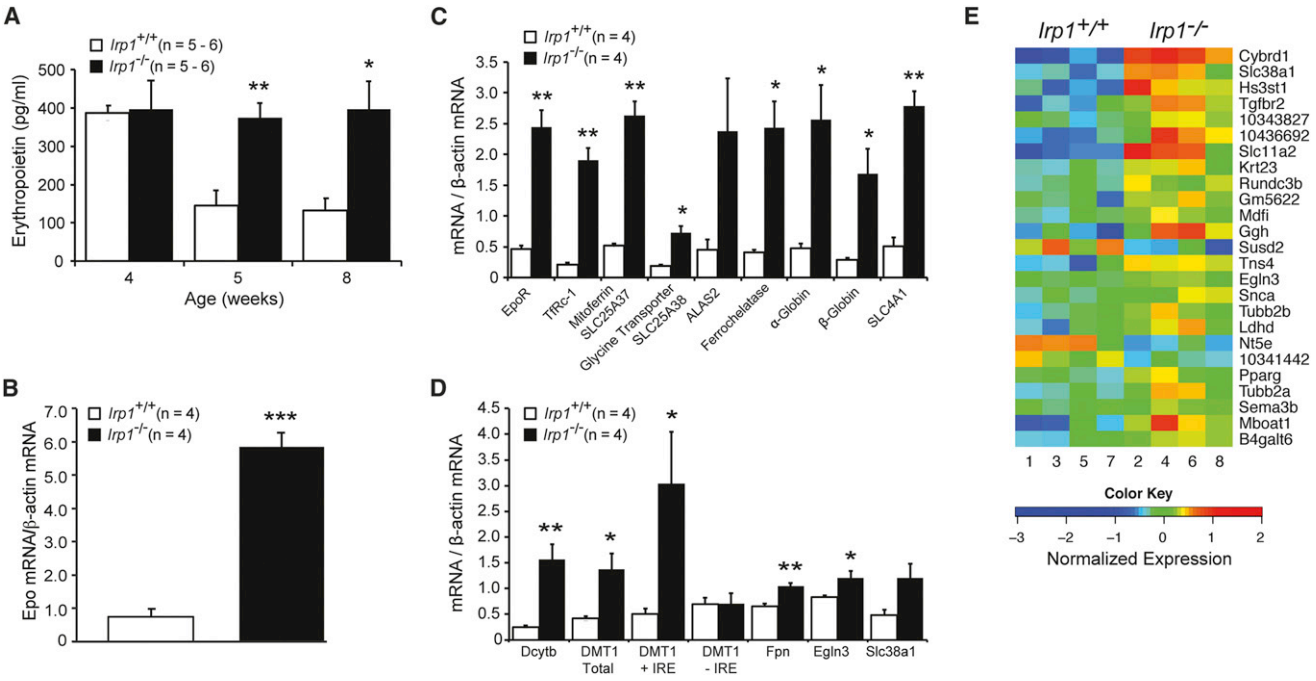

Figure 3. HIF-2α Hyperactivity in IRP1-Deficient Mice

(A) Serum Epo (pg/ml) in 4-, 5-, and 8-week-old mice.

(B) Kidney Epo messenger RNA (mRNA) level at 5 weeks.

(C) Erythroid differentiation gene mRNA levels in the spleen at 5 weeks.

(D) Duodenal mRNA level for iron transport proteins and other hypoxia-inducible factor 2α (HIF-2α) (e.g., EGLN3) targets dependent on HIF-2α for induction in iron deficiency (5 weeks).

(E) Microarray analysis of duodenal mucosal cells at 5 weeks. Response of each of four mice per genotype is shown. Posterior probability of differential expression for all genes is <0.95. Expression of five erythroid genes (globin chains α_1, α_2, β_1, β_2, and ALAS2) is not shown. Results in this figure are expressed as mean ± SEM. *, $p < 0.05$; **, $p < 0.01$; ***, $p < 0.001$.

See also Supplemental Experimental Procedures and Figure S2.

Selective Dysregulation of HIF-2α mRNA Translation in *Irp1*$^{-/-}$ Mice

To determine the basis for the development of polycythemia in *Irp1*$^{-/-}$ but not *Irp2*$^{-/-}$ mice, we determined the translation state of HIF-2α and other 5′ IRE-containing mRNAs (Figure 4 and Tables S4 and S5). Repressed mRNA in ribonucleoprotein particles (RNP) are separated from the 80S monosomes and the translationally active polysomes by polysome profile analysis. Given the increased expression of Epo mRNA in *Irp1*$^{-/-}$ kidneys, we asked whether the HIF-2α mRNA translation state was altered. In *Irp1*$^{+/+}$ kidneys, nearly equal amounts of HIF-2α mRNA were in the RNP and polysome bound pools (Figure 4A). Strikingly, in *Irp1*$^{-/-}$ but not *Irp2*$^{-/-}$ mouse kidneys, HIF-2α mRNA was substantially derepressed such that the majority was polysome-bound in comparison to those of *Irp1*$^{+/+}$ mice. Thus, IRP2 does not compensate for the absence of IRP1 in maintaining the wild-type level of repression of HIF-2α mRNA translation. Deficiency of either IRP failed to affect β-actin mRNA translation (Figure 4A). Thus, the polycythemia in *Irp1*$^{-/-}$ mice is associated with a selective translational derepression of HIF-2α mRNA in kidneys not seen in *Irp2*$^{-/-}$ mice.

Then, we investigated the role that each IRP had in controlling the translation state of 5′ IRE-containing mRNAs in the liver, a tissue in which HIF-2α has many metabolic roles (Haase, 2010). The liver expresses less IRP1-RNA binding activity in comparison to kidneys (Meyron-Holtz et al., 2004). Thus, it was not surprising that a larger fraction of HIF-2α mRNA was polysome-bound in comparison to kidneys (Figure 4B and Table S5). Similar to kidneys, loss of IRP1, but not IRP2, led to translational derepression of HIF-2α mRNA. However, all other 5′ IRE-containing mRNAs in the liver showed the opposite result. Translational derepression of H- and L-ferritin, ferroportin, and mitochondrial aconitase mRNAs was observed in *Irp2*$^{-/-}$ but not in *Irp1*$^{-/-}$ livers (Figure 4B and Table S5). Altogether, our findings illustrate unique roles for each IRP in orchestrating the fate of 5′ IRE-containing mRNAs.

Next, we asked whether the selective dysregulation of HIF-2α in *Irp1*$^{-/-}$ mice related to the level or selectivity of IRP1 and IRP2 binding activity in kidneys. Previous studies in 786-O cells found that the level of IRP2 expressed was insufficient to bind to the HIF-2α IRE (Zimmer et al., 2008). Kidney cytosol extracts from *Irp1*$^{-/-}$ or *Irp2*$^{-/-}$ mice were the source of IRP2 or IRP1, respectively, in electrophoretic mobility shift assays (Figure 4C). HIF-2α IRE binds to IRP1 as well or better than the L-ferritin IRE (Figure 4C, subpanels 1 and 2). Consistent with previous studies, IRP2 binding activity was much lower than that of IRP1 in kidneys (Meyron-Holtz et al., 2004). However, in contrast to IRP1, IRP2 bound to the L-ferritin IRE better than it did to the HIF-2α IRE.

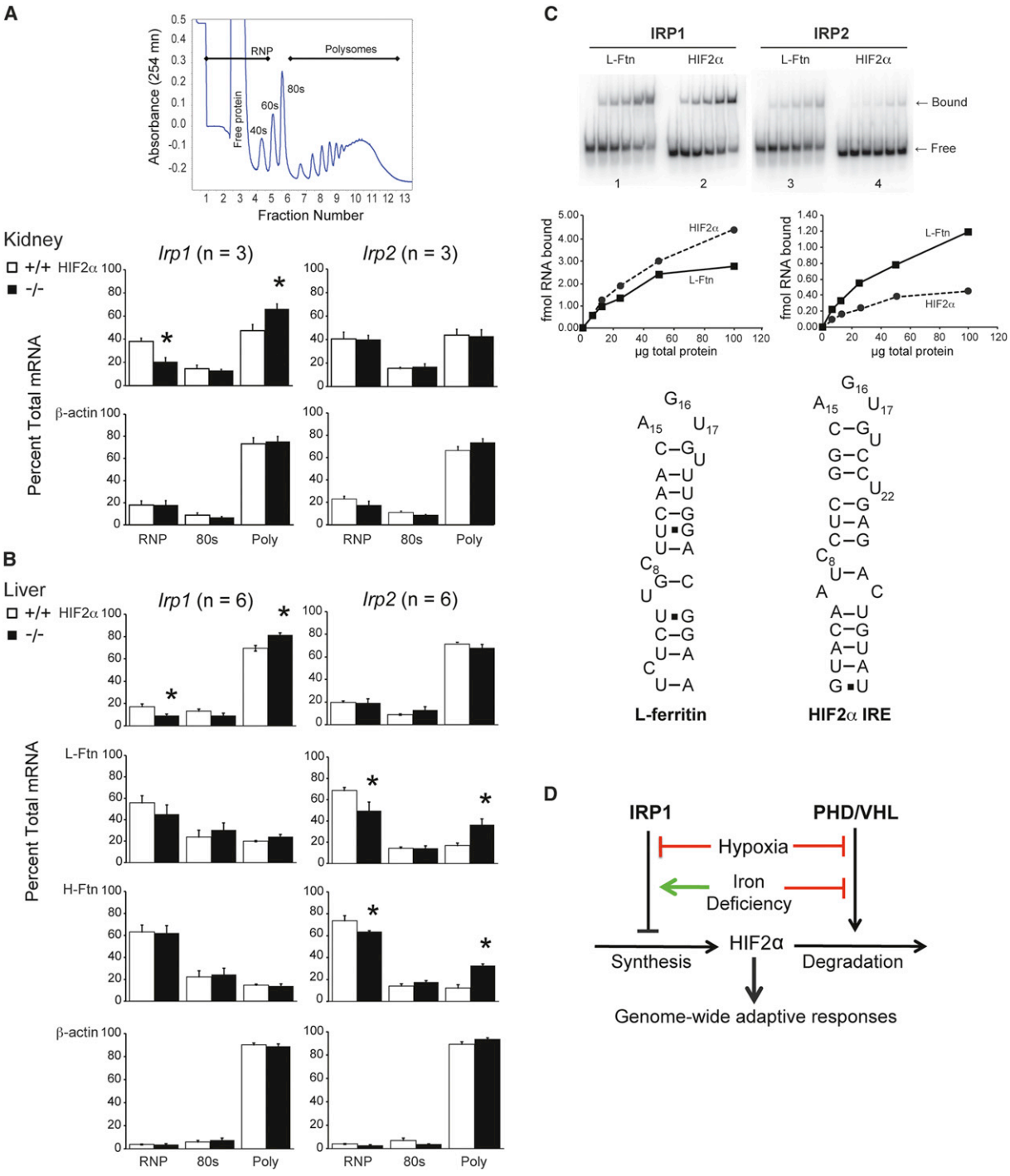

Figure 4. Selective Dysregulation of HIF-2α mRNA Translation in *Irp1*$^{-/-}$ Mice

(A) Kidney polysome profile (PP) analysis at 8 weeks. A typical PP is shown.

(B) Liver PP analysis at 8 weeks.

(C) Electrophoretic mobility shift assays from *Irp2*$^{-/-}$ or *Irp1*$^{-/-}$ kidney cytosol. Panels (1) and (2) show binding of RNAs (0.5 nM) with the use of *Irp2*$^{-/-}$ kidney cytosol, therefore binding is to IRP1. Panels (3) and (4) show binding of RNAs (0.5 nM) with the use of *Irp1*$^{-/-}$ kidney cytosol, therefore binding is to IRP2. Result is representative of n = 2 experiments. A proposed secondary structure of L-ferritin and HIF-2α IRE is also shown.

(D) Model of the impact of IRP1 on HIF-2α regulation. Results in panels (A) and (B) are expressed as mean ± SEM. *, $p < 0.05$; **, $p < 0.01$; ***, $p < 0.001$.

See also Tables S4 and S5.

Thus, the specific derepression of HIF-2α mRNA in *Irp1*$^{-/-}$ mice is associated with a reduced level of IRP2-RNA binding activity in kidneys in comparison to IRP1 coupled with a greater preference of IRP2 for the L-ferritin IRE.

Our study adds an important component to the existing paradigms concerning the integrated regulation of iron and oxygen metabolism in mammals. First, the polycythemic phenotype of *Irp1*$^{-/-}$ mice illustrates that control of HIF-2α synthesis is a major aspect of IRP1 function. A key consequence of this is that IRP1 will amplify the impact of prolyl hydroxylase-mediated regulation of HIF-2α accumulation in response to oxygen while dampening the action of iron (Figure 4D). Given that the *Irp1*$^{-/-}$ mice used here were fed a normal diet under normoxic conditions, altered exposure to iron or oxygen will most likely exacerbate the phenotype of IRP1 deficiency. Second, IRP1 has a physiologic role separable from IRP2 that suggests that IREs can be functionally distinct in vivo. The presence of a similar noncanonical 3′ unpaired nucleotide in the DMT1 IRE, as is predicted for HIF-2α (Figure 4C), and its preferential recognition by IRP1 suggest a mechanism for IRP selectivity (Gunshin et al., 2001). Third, the key role of the Fe-S switch in controlling IRP1 RNA binding activity predicts unanticipated links between major pathways of iron metabolism (e.g., Fe-S cluster biogenesis), HIF-2α, and oxygen sensing that when perturbed may contribute to disease phenotypes. Fourth, the finding that the oxygen sensitivity of the Fe-S switch mechanism of IRP1 may be modulated by S138 phosphorylation suggests critical mechanisms that may contribute to pathological abnormalities in Epo expression or other aspects of HIF-2α action (Andrews and Bridges, 1998; Deck et al., 2009; van der Putten et al., 2008).

The sensing of oxygen and iron is a central aspect of the homeostatic responses in a wide spectrum of physiological scenarios and its dysregulation is a pathophysiological feature of diseases, including polycythemias and other erythropoietic diseases, pulmonary syndromes, renal disease, cancers, and other disorders (Prabhakar and Semenza, 2012). Although HIF-2α and IRP1 respond to hypoxia, iron deficiency, and other metabolic stresses, the extent to which they do so in a concerted manner has only recently come into greater focus (Taylor et al., 2011; Zimmer et al., 2010). The current demonstration that IRP1 is the key IRP regulator of HIF-2α establishes a broad framework through which the regulation of iron and oxygen homeostasis is integrated and provides an important paradigm for defining how maladaptive regulation of this network contributes to human diseases.

EXPERIMENTAL PROCEDURES

Mice

The generation of tissue-wide *Irp1*$^{-/-}$ and *Irp2* $^{-/-}$ mice has been described previously (Galy et al., 2005a). *Irp1*$^{-/-}$ and *Irp2*$^{-/-}$ mice used here were backcrossed six generations with C57BL/6 mice. *Irp1*$^{+/-}$ or *Irp2*$^{+/-}$ mice were bred to generate *Irp1*$^{-/-}$ and *Irp2*$^{-/-}$ mice and their wild-type littermates. Animal use met the requirements of the University of Wisconsin-Madison Institutional Animal Care and Use Committee.

Hematologic and Iron Parameters

Blood was drawn from the retroorbital sinuses or hearts for complete blood count (CBC) analysis, for calculated or manual hematocrit analysis, or for serum for the Epo quantikine ELISA kit (MEP00B; R&D Systems). For CBC and hematocrit analyses, blood was collected into heparin- or EDTA-treated tubes. CBC analysis was performed at the University of Wisconsin-Madison School of Vetrinary Medicine. Blood and tissue were analyzed for serum iron or tissue nonheme iron as described previously (Schmidt et al., 2010).

Flow Cytometry

For hematopoietic cell lineage analysis, flow cytometric analyses were performed as described previously (Socolovsky et al., 2001; Zhang et al., 2009). LSK cells and myeloid progenitors were also determined by flow cytometry (Wang et al., 2011). Stained cells were analyzed on a FACSCalibur flow cytometer (BD Biosciences) or on a MACS Quant Analyzer (Miltenyi Biotec). Colony-forming assays for the quantization of BFU-E and various CFU progenitors and Epo sensitivity of CFU-E used growth in methylcellulose with defined media (STEMCELL Technologies). The antibodies directed against cell-surface antigens and other details of the flow cytometry procedure are described in the Supplemental Experimental Procedures.

Tissue Staining and Immunohistochemistry

Spleens were fixed in 10% buffered formalin and embedded in paraffin. Deparaffinized sections of tissue were stained with hematoxylin and eosin or CD71 antibody (TfR1) at the Children's Hospital Boston Department of Pathology Histology Lab. Images were acquired with the use of a 4×/0.13 objective lens on a BX51 microscope with a DP71 Digital Camera with the use of Olympus MicroSuite FIVE Imaging Software.

PCR Analysis

RNA was isolated with the use of RNA STAT-60 (Tel-Test). Reverse-transcription used total RNA, Superscript III (Invitrogen), and random hexamers. Real-time PCR on complementary DNA used SYBR Green PCR Master Mix (Applied Biosystems) on an ABI 7000.

Polysome Profile Analysis

Tissues were minced and homogenized in 3 volumes of polysome buffer (PB) (40 mM HEPES [pH 7.4], 100 mM Cl, 5 mM $MgCl_2$, 2 mM citrate, and 1 mM DTT) in a Potter-Elvehjem homogenizer. The homogenate was centrifuged at 5000 × g at 4°C for 20 min. The upper two-thirds of the supernatant was brought to 1% Na deoxycholate, 1% Triton X-100 in PB. A 500 μl sample was loaded on a linear 15%-to-60% sucrose gradient in PB and centrifuged at 180,000 × g in a Sorvall TH641 rotor for 2 hr at 4°C. Gradient fractionation used an ISCO UA-6 and 254 nm detector linked to an Agilent integrator.

Electrophoretic Mobility Shift Assays

An RNA binding assay with [^{32}P] IREs (~15,000 dpm 15,000 dpm/fmol) was performed as described previously (Goforth et al., 2010).

Microarray

Mice were fasted overnight and killed under isoflurane. Total RNA was isolated from frozen duodenal mucosal cells (see PCR Analysis), labeled with the use of the Ambion Gene Chip WT Expression Kit (Ambion), and hybridized to Affymetrix Mouse Gene 1.0 ST Arrays.

Statistical Methods

Group means were tested for differences by Student's t tests. Error bars represent SEM. Statistical analysis of arrays is described in the Supplemental Experimental Procedures.

SUPPLEMENTAL INFORMATION

Supplemental Information contains Supplemental Experimental Procedures, two figures, and six tables and can be found with this article online at http://dx.doi.org/10.1016/j.cmet.2013.01.007.

ACKNOWLEDGMENTS

This study was supported by the National Institutes of Health (NIH; R01 DK66600), the Iron Metabolism Research Fund, and the University of Wisconsin-Madison Graduate School and Hatch Project (WIS01324) to R.E.; NIH R01CA152108, a Shaw Scientist Award from the Greater Milwaukee Foundation, a V Scholar Award from the V Foundation for Cancer Research, and an

Investigator Initiated Grant from the University of Wisconsin Comprehensive Cancer Center Support (UWCCC) to J.Z.; NIH R01 DK 080011 to M.D.F.; NIH R01 GM102756 to C.K.; and a grant from the Clinical and Translational Science Award program of the National Center for Research Resources, NIH (1UL1RR025011). We thank UWCCC for use of its flow cytometry and experimental pathology units. Partial support from NIH and National Cancer Institute (P30 CA014520) was also given to the UWCCC.

Received: August 25, 2012
Revised: November 19, 2012
Accepted: January 14, 2013
Published: February 7, 2013

REFERENCES

Anderson, C.P., Shen, M., Eisenstein, R.S., and Leibold, E.A. (2012). Mammalian iron metabolism and its control by iron regulatory proteins. Biochim. Biophys. Acta *1823*, 1468–1483.

Andrews, N.C., and Bridges, K.R. (1998). Disorders of iron metabolism and sideroblastic anemia. In Nathan and Oski's Hematology in Infancy and Childhood, D.G. Nathan and S.H. Oski, eds. (Philadelphia, PA: W.B. Saunders), pp. 423–461.

Bullock, G.C., Delehanty, L.L., Talbot, A.L., Gonias, S.L., Tong, W.H., Rouault, T.A., Dewar, B., Macdonald, J.M., Chruma, J.J., and Goldfarb, A.N. (2010). Iron control of erythroid development by a novel aconitase-associated regulatory pathway. Blood *116*, 97–108.

Cooperman, S.S., Meyron-Holtz, E.G., Olivierre-Wilson, H., Ghosh, M.C., McConnell, J.P., and Rouault, T.A. (2005). Microcytic anemia, erythropoietic protoporphyria, and neurodegeneration in mice with targeted deletion of iron-regulatory protein 2. Blood *106*, 1084–1091.

Davis, M.R., Shawron, K.M., Rendina, E., Peterson, S.K., Lucas, E.A., Smith, B.J., and Clarke, S.L. (2011). Hypoxia inducible factor-2 α is translationally repressed in response to dietary iron deficiency in Sprague-Dawley rats. J. Nutr. *141*, 1590–1596.

Deck, K.M., Vasanthakumar, A., Anderson, S.A., Goforth, J.B., Kennedy, M.C., Antholine, W.E., and Eisenstein, R.S. (2009). Evidence that phosphorylation of iron regulatory protein 1 at Serine 138 destabilizes the [4Fe-4S] cluster in cytosolic aconitase by enhancing 4Fe-3Fe cycling. J. Biol. Chem. *284*, 12701–12709.

Franovic, A., Holterman, C.E., Payette, J., and Lee, S. (2009). Human cancers converge at the HIF-2α oncogenic axis. Proc. Natl. Acad. Sci. USA *106*, 21306–21311.

Galy, B., Ferring, D., and Hentze, M.W. (2005a). Generation of conditional alleles of the murine Iron Regulatory Protein (IRP)-1 and -2 genes. Genesis *43*, 181–188.

Galy, B., Ferring, D., Minana, B., Bell, O., Janser, H.G., Muckenthaler, M., Schümann, K., and Hentze, M.W. (2005b). Altered body iron distribution and microcytosis in mice deficient in iron regulatory protein 2 (IRP2). Blood *106*, 2580–2589.

Goforth, J.B., Anderson, S.A., Nizzi, C.P., and Eisenstein, R.S. (2010). Multiple determinants within iron-responsive elements dictate iron regulatory protein binding and regulatory hierarchy. RNA *16*, 154–169.

Gruber, M., Hu, C.J., Johnson, R.S., Brown, E.J., Keith, B., and Simon, M.C. (2007). Acute postnatal ablation of Hif-2α results in anemia. Proc. Natl. Acad. Sci. USA *104*, 2301–2306.

Gunshin, H., Allerson, C.R., Polycarpou-Schwarz, M., Rofts, A., Rogers, J.T., Kishi, F., Hentze, M.W., Rouault, T.A., Andrews, N.C., and Hediger, M.A. (2001). Iron-dependent regulation of the divalent metal ion transporter. FEBS Lett. *509*, 309–316.

Haase, V.H. (2010). Hypoxic regulation of erythropoiesis and iron metabolism. Am. J. Physiol. Renal Physiol. *299*, F1–F13.

Hattangadi, S.M., Wong, P., Zhang, L., Flygare, J., and Lodish, H.F. (2011). From stem cell to red cell: regulation of erythropoiesis at multiple levels by multiple proteins, RNAs, and chromatin modifications. Blood *118*, 6258–6268.

Hentze, M.W., Muckenthaler, M.U., Galy, B., and Camaschella, C. (2010). Two to tango: regulation of mammalian iron metabolism. Cell *142*, 24–38.

Keith, B., Johnson, R.S., and Simon, M.C. (2012). HIF1α and HIF2α: sibling rivalry in hypoxic tumor growth and progression. Nat. Rev. Cancer. *12*, 9–22.

Lee, F.S., and Percy, M.J. (2011). The HIF pathway and erythrocytosis. Annu. Rev. Pathol. *6*, 165–192.

Majmundar, A.J., Wong, W.J., and Simon, M.C. (2010). Hypoxia-inducible factors and the response to hypoxic stress. Mol. Cell *40*, 294–309.

Mastrogiannaki, M., Matak, P., Keith, B., Simon, M.C., Vaulont, S., and Peyssonnaux, C. (2009). HIF-2α, but not HIF-1α, promotes iron absorption in mice. J. Clin. Invest. *119*, 1159–1166.

Meyron-Holtz, E.G., Ghosh, M.C., Iwai, K., LaVaute, T., Brazzolotto, X., Berger, U.V., Land, W., Ollivierre-Wilson, H., Grinberg, A., Love, P., et al. (2004). Genetic ablations of iron regulatory proteins 1 and 2 reveal why iron regulatory protein 2 dominates iron homeostasis. EMBO J. *23*, 386–395.

Minamishima, Y.A., Moslehi, J., Padera, R.F., Bronson, R.T., Liao, R., and Kaelin, W.G., Jr. (2009). A feedback loop involving the Phd3 prolyl hydroxylase tunes the mammalian hypoxic response in vivo. Mol. Cell. Biol. *29*, 5729–5741.

Pescador, N., Cuevas, Y., Naranjo, S., Alcaide, M., Villar, D., Landázuri, M.O., and Del Peso, L. (2005). Identification of a functional hypoxia-responsive element that regulates the expression of the egl nine homologue 3 (*Egln3*/*Phd3*) gene. Biochem. J. *390*, 189–197.

Peslak, S.A., Wenger, J., Bemis, J.C., Kingsley, P.D., Koniski, A.D., McGrath, K.E., and Palis, J. (2012). EPO-mediated expansion of late-stage erythroid progenitors in the bone marrow initiates recovery from sublethal radiation stress. Blood *120*, 2501–2511.

Prabhakar, N.R., and Semenza, G.L. (2012). Adaptive and maladaptive cardiorespiratory responses to continuous and intermittent hypoxia mediated by hypoxia-inducible factors 1 and 2. Physiol. Rev. *92*, 967–1003.

Sanchez, M., Galy, B., Muckenthaler, M.U., and Hentze, M.W. (2007). Iron-regulatory proteins limit hypoxia-inducible factor-2alpha expression in iron deficiency. Nat. Struct. Mol. Biol. *14*, 420–426.

Schmidt, P.J., Andrews, N.C., and Fleming, M.D. (2010). Hepcidin induction by transgenic overexpression of Hfe does not require the Hfe cytoplasmic tail, but does require hemojuvelin. Blood *116*, 5679–5687.

Scortegagna, M., Ding, K., Zhang, Q., Oktay, Y., Bennett, M.J., Bennett, M., Shelton, J.M., Richardson, J.A., Moe, O., and Garcia, J.A. (2005). HIF-2α regulates murine hematopoietic development in an erythropoietin-dependent manner. Blood *105*, 3133–3140.

Shah, Y.M., Matsubara, T., Ito, S., Yim, S.H., and Gonzalez, F.J. (2009). Intestinal hypoxia-inducible transcription factors are essential for iron absorption following iron deficiency. Cell Metab. *9*, 152–164.

Socolovsky, M., Nam, H., Fleming, M.D., Haase, V.H., Brugnara, C., and Lodish, H.F. (2001). Ineffective erythropoiesis in Stat5a$^{(-/-)}$5b$^{(-/-)}$ mice due to decreased survival of early erythroblasts. Blood *98*, 3261–3273.

Strauss, R.G. (2010). Anaemia of prematurity: pathophysiology and treatment. Blood Rev. *24*, 221–225.

Taylor, M., Qu, A., Anderson, E.R., Matsubara, T., Martin, A., Gonzalez, F.J., and Shah, Y.M. (2011). Hypoxia-inducible factor-2α mediates the adaptive increase of intestinal ferroportin during iron deficiency in mice. Gastroenterology *140*, 2044–2055.

Tong, W.H., Sourbier, C., Kovtunovych, G., Jeong, S.Y., Vira, M., Ghosh, M., Romero, V.V., Sougrat, R., Vaulont, S., Viollet, B., et al. (2011). The glycolytic shift in fumarate-hydratase-deficient kidney cancer lowers AMPK levels, increases anabolic propensities and lowers cellular iron levels. Cancer Cell *20*, 315–327.

van der Putten, K., Braam, B., Jie, K.E., and Gaillard, C.A. (2008). Mechanisms of Disease: erythropoietin resistance in patients with both heart and kidney failure. Nat. Clin. Pract. Nephrol. *4*, 47–57.

Wang, J., Liu, Y., Li, Z., Wang, Z., Tan, L.X., Ryu, M.J., Meline, B., Du, J., Young, K.H., Ranheim, E., et al. (2011). Endogenous oncogenic Nras mutation initiates hematopoietic malignancies in a dose- and cell type-dependent manner. Blood *118*, 368–379.

Weiss, G., and Goodnough, L.T. (2005). Anemia of chronic disease. N. Engl. J. Med. *352*, 1011–1023.

Young, R.M., Wang, S.J., Gordan, J.D., Ji, X., Liebhaber, S.A., and Simon, M.C. (2008). Hypoxia-mediated selective mRNA translation by an internal ribosome entry site-independent mechanism. J. Biol. Chem. *283*, 16309–16319.

Zhang, J., Wang, J., Liu, Y., Sidik, H., Young, K.H., Lodish, H.F., and Fleming, M.D. (2009). Oncogenic Kras-induced leukemogeneis: hematopoietic stem cells as the initial target and lineage-specific progenitors as the potential targets for final leukemic transformation. Blood *113*, 1304–1314.

Zimmer, M., Ebert, B.L., Neil, C., Brenner, K., Papaioannou, I., Melas, A., Tolliday, N., Lamb, J., Pantopoulos, K., Golub, T., and Iliopoulos, O. (2008). Small-molecule inhibitors of HIF-2a translation link its 5'UTR iron-responsive element to oxygen sensing. Mol. Cell *32*, 838–848.

Zimmer, M., Lamb, J., Ebert, B.L., Lynch, M., Neil, C., Schmidt, E., Golub, T.R., and Iliopoulos, O. (2010). The connectivity map links iron regulatory protein-1-mediated inhibition of hypoxia-inducible factor-2a translation to the anti-inflammatory 15-deoxy-delta12,14-prostaglandin J2. Cancer Res. *70*, 3071–3079.